

Josephson effects in  $\text{MgB}_2$  metal-masked ion damage junctionsD.-J. Kang<sup>y</sup>

Department of Materials Science, University of Cambridge,  
 Pembroke Street, Cambridge CB2 3QZ, UK

N. H. Peng, R. Webb, and C. Jeynes

Surrey Centre for Research in Ion Beam Applications,  
 School of Electronics, Computing and Mathematics,  
 University of Surrey, Guildford, GU2 7XH, UK

J. H. Yun, S. H. Moon, and B. Oh

LG Electronics Institute of Technology, Seoul 137-724, Korea

G. Bumell, E. J. Tarte, D. F. Moore, and M. G. Blamire

IRC in Superconductivity, University of Cambridge,  
 Madingley Road, Cambridge CB3 0HE, UK

(Dated: April 14, 2024)

## Abstract

Ion beam damage combined with nanoscale focused ion beam direct milling was used to create manufacturable SNS type Josephson junctions in 100 nm thick  $\text{MgB}_2$  with  $T_C$  of 38 K. The junctions show non-hysteretic current-voltage characteristics between 36 and 4.2 K. Experimental evidence for the dc and ac Josephson effects in  $\text{MgB}_2$  metal-masked ion damage junctions are presented. This technique is particularly useful for prototyping devices due to its simplicity and flexibility of fabrication and has a great potential for high-density integration.

---

<sup>y</sup>D.-J. Kang is also with IRC for Nanotechnology, University of Cambridge, Cambridge CB3 0HE, UK.

The recent discovery of superconductivity in  $\text{MgB}_2$  at 39 K<sup>1</sup> is of both fundamental and practical importance due to the material's attractive properties, including relatively isotropic superconductivity, large coherence lengths, transparency of grain boundaries to current flow and the highest transition temperature ( $T_c$ ) found in a simple compound. Both for applications and basic studies, extensive efforts<sup>2,3,4,5,6,7</sup> to realize a viable junction fabrication technology have been made worldwide. Unfortunately, however, the fabrication of Josephson junctions in thin  $\text{MgB}_2$  films has turned out to be rather difficult because of the relatively poor fabrication control and lack of suitable barrier materials for any multilayer type junctions, as well as the technical challenge of realizing high quality thin films.

Nb-based junctions, with a typical  $J_c$  of only around 1 kA/cm<sup>2</sup> have a Stewart-McCumber parameter,  $\beta_c$  which is much larger than 1. As a result, the junctions have a hysteretic current-voltage ( $I-V$ ) characteristics, and for application in dc SQUIDs and RSFQ logic gates they must be externally shunted to decrease the effective value of  $\beta_c$ . Furthermore, maximum clock speed of simple microprocessor that can be made using such Nb junctions seems to be limited to less than 25 GHz.<sup>8</sup> This number is barely competitive with the current-state-of-art complementary metal oxide semiconductor and SiGe heterojunction bipolar transistor technologies for high-performance digital signal processing and general-purpose computing, even without the burdens of helium cooling for the operation. However,  $\text{MgB}_2$ , has the potential to overcome these limitations as the material is found to be able to carry much larger  $J_c$ , and its  $T_c$  is about two times higher than that of the Nb-based superconductors. This allows one to work safely above 20 or even 30 K, which is comparatively easy with standard cryocoolers.

Ion irradiation has the potential to be used as a means to modify superconducting properties as well as to create superconducting weak links. Bugoslavsky et al.<sup>9</sup> recently showed that the superconducting properties of  $\text{MgB}_2$  can be strongly affected by defects and structural disorder created by high energy ion irradiation. Fabrication of junctions without interfaces, i.e.: weakened structures, by ion or electron irradiation<sup>10,11</sup> is particularly attractive due to its controllability.

In this letter, we report the successful creation of SNS type  $\text{MgB}_2$  junctions by localized ion implantation. The junctions display non-hysteretic current-voltage ( $I-V$ ) characteristics between 36 and 4.2 K. Microwave-induced steps and an oscillatory magnetic field dependence of  $I_c$  were observed. Junctions on the same chip show nearly identical proper-

ties. The junction parameters were found to be highly controllable through careful in-situ monitoring of resistance change during ion irradiation and subsequent rapid thermal annealing (RTA) step.

The films used were 20 nm Au/100 nm MgB<sub>2</sub> bilayer thin films grown on (0001) sapphire substrates; details of the growth has been described elsewhere.<sup>12</sup> 20 nm thick Au was deposited to protect the MgB<sub>2</sub> films from degradation during storage before further processing steps. An additional 430 nm of Au was ex situ deposited by dc magnetron sputtering on top of the 20 nm of Au for use as a hard mask during the ion irradiation step. Tracks 3  $\mu$ m wide and contacts were then patterned by standard optical lithography and broad beam Ar ion milling at 500 V and 10 mA current on a water-cooled rotating stage. The T<sub>c</sub> of the tracks was measured before and after photolithography and was found to be unchanged at around 38 K.

In order to prepare metal mask apertures, the patterned chip was transferred to the FIB microscope (Philips Electron Optics/FEI Corporation 200 xP<sup>®</sup> FIB workstation) with a Ga source. The aperture was defined by writing a single pixel line cut across the width of tracks using a 4 pA 30 kV Ga ion beam. The chip was wire-bonded to enable in-situ monitoring of the resistance change during the FIB milling process to provide us with accurate cutting depth.<sup>13</sup>

After the metal mask apertures were prepared, the sample was mounted on an ion implanter equipped with a custom cryogenic stage and shielded to allow ion implantation of the device through a 2 mm aperture. While monitoring the barrier resistance in-situ, the chips were then exposed to a 100 keV H<sub>2</sub><sup>+</sup> ion beam with a nominal dose of up to 1 x 10<sup>16</sup> ions/cm<sup>2</sup> at 20 K. This temperature was chosen to ensure that the intended maximum operating temperature of the completed devices is close to the T<sub>c</sub> of the bulk after subsequent RTA processing. RTA was carried out at 300 °C for 1 min following a ramp of 60 s. More detailed information on this ion damage technology has been published elsewhere.<sup>14,15</sup>

Basic junction characterization was performed between 4.2 K and T<sub>c</sub> using a dip probe including magnetic field coils and microwave antenna. I-V characteristics were obtained in a quasi-static current-biased measurement. Microwave measurements were done in the range of 12 – 18 GHz.

Figure 1 shows resistance versus temperature measurements for the same track before (a) and after ion implantation (b). It is clear from the figure that FIB processing has no

significant effect on  $T_c$ . However, the sharp peak just before the transition region of the sample was observed after the chip was irradiated at 20 K. This feature can be ascribed to a current redistribution along the bilayer voltage leads just before entering the superconducting phase.

Figure 2 shows the temperature dependence of critical current ( $I_c$ ) and normal resistance ( $R_n$ ) of the junctions. The  $R_n$  was nearly temperature-independent between 36 and 42 K and was about 0.114  $\Omega$  at 42 K. This and the temperature dependency of the  $I_c$  give evidence for SNS nature of the junctions. The inset in Fig. 2 is an example of  $I$ - $V$  characteristics of the junction at 42 K. The  $I$ - $V$  characteristics shows resistively shunted junction (RSJ) model behavior with some excess current. In this case, we have  $I_c = 6.5$  mA ( $J_c = 2.17$  MA/cm<sup>2</sup>) and  $R_n = 0.114$   $\Omega$  from which a product  $I_c R_n = 0.69$  mV is obtained. This value is still small if compared with the value  $I_c R_n = \Phi_0/2 = 3.52$   $k_B T_c/4 = 9.3$  mV predicted by the BCS theory for  $T_c = 39$  K. No significant change in the junction properties was observed over 2 months and a number of thermal cycles.

Figure 3 shows the magnetic modulation of the  $I_c$  of a junction at 34 K. Deviation from the ideal Fraunhofer diffraction at high magnetic field in the experimental data implies that some inhomogeneities exist in local areas of the junction. However, the data clearly indicates that our barrier shows a good Josephson junction behavior. The apparently incomplete suppression of the  $I_c$  is largely due to the fixed voltage criterion used to assess the  $I_c$ . We found, however that there is genuinely an excess critical current for all applied magnetic fields. The asymmetry and hysteresis of the  $I_c$  modulation is probably a consequence of an asymmetrical current distribution due to some unevenness in the cut made in the mask, or flux trapped during the long measurement times. The nodes in the critical current occur every 2 mT. The value of London penetration depth ( $\lambda_L$ ) in our irradiated junctions can be obtained from the  $I_c(B)$  curve by means of the flux density expression  $B = \Phi_0/(2\lambda_L + l)w$  where  $\Phi_0$  is the flux quantum,  $l$  is the length of junction barrier, and  $w$  is the width of the junction, assuming flux focusing effects are negligible for a junction of this size. We found that  $\lambda_L$  of MgB<sub>2</sub> was approximately 150 nm. This is in good agreement with values reported elsewhere.<sup>16,17,18</sup>

To further examine the Josephson effect, 12 GHz microwave were applied to the junction. Shapiro steps were observed at the expected voltages ( $V = h/2e \cdot 25$  V) as shown in Fig. 4 despite the low normal resistance of the junction due to screening by the thick Au mask

layer. It is also likely that such a thick Au mask layer (450 nm) on the top of the junction barrier will attenuate the interaction between the junction and microwave radiation. At the frequency ( $\sim 12$  GHz), the skin depth of Au is only around 680 nm, which is just 1.55 times thicker than the mask.

Improvement in the junction quality following the RTA procedure is illustrated by comparing an  $I_c(B)$  curve without RTA (Fig. 3 inset) with that after RTA (Fig. 3, main). RTA was taken to facilitate annealing of most of the low energy defects and to trap the core defects within a narrow region forming the junction barrier. Therefore, a reduction in the effective lateral extension of the defect profile should be expected as well.<sup>9</sup> However, even though we have shown here the successful creation of Josephson junctions on the MgB<sub>2</sub>, precise mechanism is still unclear.

In conclusion, we have reported the successful creation of MgB<sub>2</sub> junctions by localized ion implantation in combination with focused ion beam direct milling. The junctions show non-hysteretic  $I-V$  characteristics between 3.6 and 4.2 K. Clear dc and ac Josephson effects in MgB<sub>2</sub> metal masked ion damaged junctions were observed. The product  $I_c R_n$  of our junctions is small compared to the BCS value but critical currents up to 6.5 mA at 4.2 K were observed. This technique holds a promise for prototyping devices due to its simplicity and flexibility of fabrication and has a great potential for high-density integration.

This work was supported by the UK Engineering and Physical Sciences Research Council. H. N. Lee, S. H. Moon and B. Oh are grateful to the Korean Ministry of Science and Technology under the National Research Laboratory project for support.

- 
- <sup>y</sup> Electronic address: djk1003@cam.ac.uk
- <sup>1</sup> J. Nagamatsu, N. Nakagawa, T. M. Iwamura, Y. Zenitani, and J. Akimitsu, *Nature* 410, 63 (2001).
- <sup>2</sup> R. S. Gonnelli, A. Calzolari, D. Daghero, G. A. Ummarino, V. A. Stepanov, G. Giunchi, S. Ceresara and G. Ripamonti, *Phys. Rev. Lett.* 87 097001 (2001).
- <sup>3</sup> A. Brinkman, D. Veldhuis, D. Mijatovic, G. Rijnders, D. H. A. Blank, H. Hilgenkamp and H. Rogalla, *Appl. Phys. Lett.* 79 2420 (2001).
- <sup>4</sup> Y. Zhang, D. K. Inou, J. Chen, D. G. Hinks, G. W. Crabtree and J. Clarke, *Phys. Rev. Lett.* (2001).
- <sup>5</sup> Z.-Z. Li, Y. Kuan, H.-J. Tao, Z.-A. Ren, G.-C. Che, B.-R. Zhao and Z.-X. Zhao, *Supercond. Sci. Tech.* 14 944 (2001).
- <sup>6</sup> G. Bumell, D.-J. Kang, H. N. Lee, S. H. Moon, B. Oh and M. G. Blamire, *Appl. Phys. Lett.* 79 (21), 3464, (2001).
- <sup>7</sup> G. Bumell, D.-J. Kang, D. A. Ansell, H. N. Lee, S. H. Moon, E. J. Tarte and M. G. Blamire, in press, *Appl. Phys. Lett.* (2002).
- <sup>8</sup> M. Dorjrev, P. Bunyk and D. Zinoviev, *IEEE Trans. Supercond.* Vol.11, no. 1, 326-332 (2001).
- <sup>9</sup> Y. Bugoslavsky, G. K. Perkins, X. Qi, L. F. Cohen and A. D. Caplin, *Nature* 410, 563 (2001).
- <sup>10</sup> S. S. Tinchov, *Supercond. Sci. Technol.* 12 L5, (1999).
- <sup>11</sup> W. E. Booi, A. J. Pauza, E. J. Tarte, D. F. Moore and M. G. Blamire, *Phys. Rev. B* 55, 14600 (1997).
- <sup>12</sup> S. H. Moon, J. H. Yun, H. N. Lee, J. I. Kye, H. G. Kim, W. Chung and B. Oh, *Appl. Phys. Lett.* 79 599 (2001).
- <sup>13</sup> A. Latif, W. E. Booi, J. H. Durrell and M. G. Blamire, *J. Vac. Sci. Technol. B* 18, 761, (2000).
- <sup>14</sup> D.-J. Kang, G. Bumell, S. J. Lloyd, R. S. Speaks, N. H. Peng, C. Jeynes, R. Webb, J. H. Yun, S. H. Moon, B. Oh, E. J. Tarte, D. F. Moore and M. G. Blamire, *Appl. Phys. Lett.* 80, 814 (2002).
- <sup>15</sup> D.-J. Kang, N. H. Peng, C. Jeynes, R. Webb, J. H. Yun, S. H. Moon, B. Oh, G. Bumell, E. J. Tarte, D. F. Moore and M. G. Blamire, in press, *Nuc. Inst. Meth. B* (2002).
- <sup>16</sup> X. H. Chen, Y. Y. Xue, R. L. Meng and C. W. Chu (unpublished)

- <sup>17</sup> D . K . Finnem ore, J . E . O stenson, S . L . Bud'ko, G . Lapertot and P . C . Can eld, Phys. Rev. Lett. 86, 2420, (2001).
- <sup>18</sup> Y . Takano, H . Takeya, H . Fuji, H . Kum akura, T . Hatano, K . Togano, H . K ito and H . Ihara, Appl Phys. Lett. 78, 2914, (2001).
- <sup>19</sup> F . K ahm ann, A . Engelhardt, J . Schubert, W . Zander and Ch . Buchal, Appl Phys. Lett. 73, 2354, (1998).

## Figure Captions

Fig. 1. Resistance versus temperature measurements for the same track of  $\text{MgB}_2$  before (a) and after ion implantation (b).

Fig. 2. The temperature dependence of  $I_c$  and  $R_n$  of a junction. Inset:  $I-V$  characteristics of a junction at 4.2 K.

Fig. 3. Critical current versus magnetic field for a device measured at 34 K. Inset shows critical current versus magnetic field measurement for a device that has not gone through the RTA treatment.

Fig. 4. The  $I-V$  characteristics of  $\text{MgB}_2$  junction and Shapiro steps under microwave irradiation of a frequency 12 GHz at 34 K.



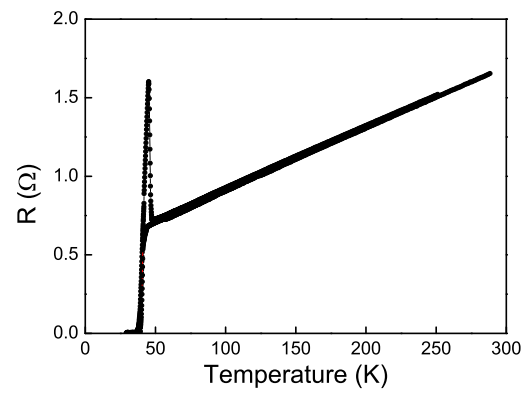


FIG .1: K ang et al.

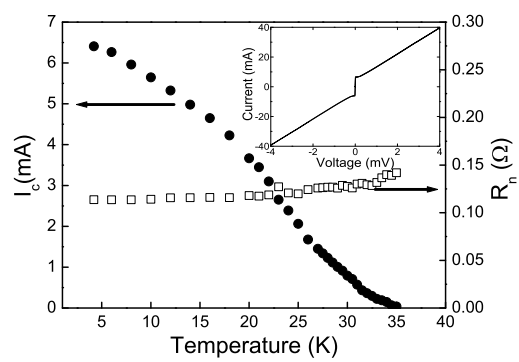


FIG. 2: Kang et al.

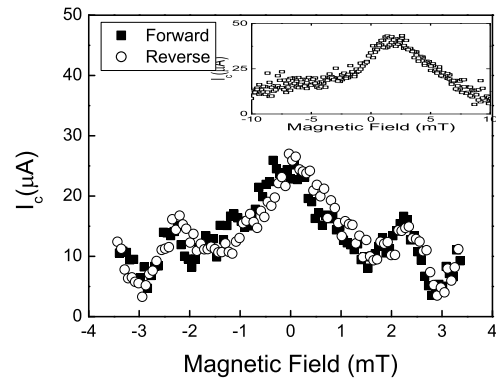


FIG. 3: Kang et al.

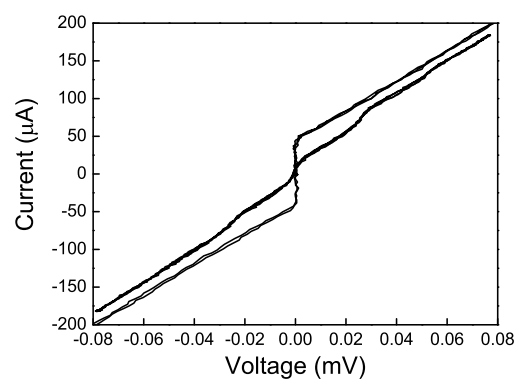


FIG .4: K ang et al.